JOURNAL OF MATERIALS SCIENCE 22 (1987) 1894–1900

The diffusion-controlled dissolution of spheres

M. CABLE, J. R. FRADE
Department of Ceramics Glasses and Polymers, University of Sheffield, Sheffield S10 2TZ, UK

The partial differential equations which describe the diffusion controlled behaviour of an isolated sphere growing or dissolving in conditions of spherical symmetry are presented. These have been solved numerically by methods already shown, by comparison with analytical solutions for growth from zero size, to give accurate results for growing spheres. Computed radius–time relations, time to dissolve completely and concentration profiles are illustrated and discussed. The influences of radial motion of the boundary and convection in the liquid are considered and shown to be important even for very high solubility. The only simple approximation of any useful range of validity is the quasi-steady state model which is valid only for very low solubilities. The flat slab model which might be expected to apply for high solubilities is useful only for the early stages of dissolution because of the change in size of the sphere.

1. Introduction

The dissolution of bubbles and other nearly spherical particles is important in many scientific and technical problems and these phenomena are often controlled by diffusion. The simplest model is an isolated stationary sphere of pure solute surrounded by an infinite body of medium in which diffusion is assumed to control the behaviour of the system and spherical symmetry is maintained. The present authors have a particular interest in problems caused by gas bubbles in glass melting where the high viscosity of the melt means that rise to the surface does not rapidly remove all bubbles and growth or dissolution becomes important.

Self-similar exact solutions for one component spheres growing from zero initial size were given by Scriven [1] in the classic paper on this subject. That type of solution has recently been extended by Cable and Frade to the growth of multi-component gas bubbles [2] and to growth of spheres with concentration-dependent diffusivity [3]. No such solutions exist for the dissolution of spheres because the partial differential equations cannot be cast into the required ordinary differential form. Efficient numerical methods have therefore been developed for spheres of finite initial size and these have been carefully tested against analytical solutions for growth from zero for wide ranges of the parameters concerned [4]. In those cases transient effects, such as changes in the shape of the normalized concentration profile, persisted until spheres had grown to about four times their initial size. Such transients are thus likely to affect the whole course of dissolution.

Approximate quasi-stationary solution have been obtained for spheres of finite initial size by analogy with the equivalent heat conduction problem for a sphere of constant size [5]. These solutions are reasonably accurate for sufficiently low effective solubilities and have often been used to analyse dissolution of bubbles in liquids [6]. However, they become increasingly poor as the effective solubility increases. Quasi-stationary and quasi-steady state approximations (the latter ignoring transients and convection of solute) converge for very low solubilities but both types of approximation need to be tested against alternative more accurate solutions to establish their ranges of validity. This can be done for growing spheres by comparing approximate solutions with exact solutions for growth from zero size but only numerical solutions of the partial differential equations are possible for dissolving spheres. The accuracy of some asymptotic solutions [7] also needs to be assessed by comparison with numerical results.

Finite difference solutions have previously been obtained by a number of workers [7–10] but were not subjected to detailed tests. Sophisticated computing techniques are needed to ensure accuracy and efficiency. Implicit methods are usually superior to explicit finite difference schemes but their performance is also very dependent on the use of a suitable transformation of the space variable to immobilize the interface and choice of algorithms to select the appropriate space and time mesh sizes.

2. Statement of the problem

An isolated sphere of radius a containing a uniform and constant concentration of pure solute (c_s) is surrounded by an infinite body of liquid; temperature and pressure are constant; the liquid is uniform and spherical symmetry is maintained. Transfer of material to or from the sphere is controlled by Fickian diffusion and the dissolved concentration of solute in the liquid at the interface remains constant at c_a; the diffusivity (D) of the solute in the liquid is also constant. Any effects of surface tension, viscosity, inertia or gravity are excluded. The partial molar volumes of solute (v) and solvent are constant but not necessarily equal. In these conditions diffusion of solute in the solution is described by, if c is concentration; r, radius and t,

0022–2461/87 $03.00 + .12

time,

$$\frac{\partial c}{\partial t} = D\left[\frac{\partial^2 c}{\partial r^2} + \frac{2}{r}\frac{\partial c}{\partial r}\right] - \varepsilon\left(\frac{a}{r}\right)^2 \frac{da}{dt}\frac{\partial c}{\partial r} \quad (1)$$

where $\varepsilon = (1 - c_s v)$ is Scriven's volume change parameter and the rate of change of size of the sphere is

$$\frac{da}{dt} = \frac{D}{c_s(1 - c_a v)}\left(\frac{\partial c}{\partial r}\right)_a = \frac{D}{c_s - (1 - \varepsilon)c_a}\left(\frac{\partial c}{\partial r}\right)_a \quad (2)$$

The term $(1 - \varepsilon)$ represents the ratio of the volume occupied by a mole of solute in the solution to that which it occupies in the sphere.
The boundary and initial conditions are

$$c(a) = c_a; \quad t \geqslant 0,$$
$$c(\infty) = c_\infty; \quad t \geqslant 0,$$
$$c(r) = c_\infty; \quad r > a, t = 0.$$

Using the chosen dimensionless variables $F = (c - c_\infty)/[c_s - c_a(1 - \varepsilon)]$, $e = r/a_0$, $R = a/a_0$ and $z = Dt/a_0^2$ transforms Equations 1 and 2 into

$$\frac{\partial F}{\partial z} = \frac{\partial^2 F}{\partial e^2} + \frac{2}{e}\frac{\partial F}{\partial e} - \varepsilon\left(\frac{R}{e}\right)^2 \frac{dR}{dz}\frac{\partial F}{\partial e} \quad (3)$$

and

$$\frac{dR}{dz} = \left(\frac{\partial F}{\partial e}\right)_R, \quad (4)$$

whilst the boundary conditions become

$$F(\infty) = 0; \quad z > 0,$$
$$F(R) = F_a = (c_a - c_\infty)/[c_s - c_a(1 - \varepsilon)]; \quad z \geqslant 0,$$
$$F(e) = 0; \quad e > R; z = 0.$$

An implicit finite difference technique was employed to solve Equations 3 and 4 [11]. This method uses a transformation of the space variable into $x = e/R$ to immobilize the interface. Variable space and time mesh sizes were used and the radial mesh points were redistributed every ten time steps to keep the concentration differences less than 1% between adjacent points; as the concentration varies smoothly in the tail of the distribution, the ratio of the amplitudes of adjacent spaces was there kept below 1.25. Time increments were computed sequentially, using the rate of change of size (dR/dz) to prevent ΔR exceeding $0.01R$ but time increments were also not allowed to exceed 2% of the actual time. The initial concentration profile, corresponding to a 1% change in radius, was computed from the error function solution for a flat slab [12].

Lacking general analytical solutions for dissolving spheres, the accuracy of these techniques was verified by comparing the computed results for asymptotic growth from finite initial size with the equivalent exact solutions for growth from zero obtained by Scriven, see Cable and Frade [4]. Very close agreement was demonstrated for rate of growth, the shape of the concentration profile and overall conservation of the mass of solute transferred into the sphere, for wide ranges of the parameters involved. Since the computations are performed in terms of the space variable $x = e/R$ the method will perform just as well for a collapsing diffusion field as for an expanding one and verification for growing spheres is considered a sufficient test.

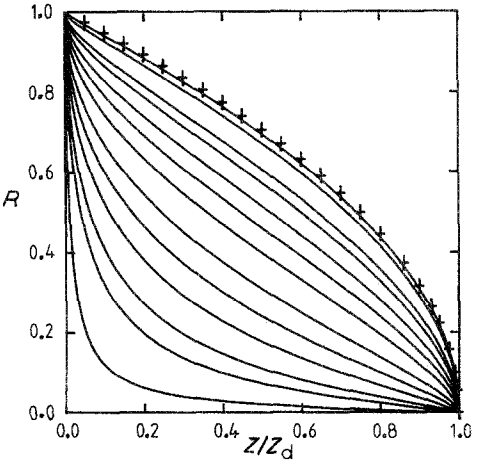

Figure 1 Normalized radius–time curves for dissolving spheres with $\varepsilon = 1$ and $F_a = 0.001, 0.01, 0.1, 0.2, 0.5, 1, 2, 5, 10, 20, 50, 100$ and 1000 (reading from top to bottom). + + + shows the quasi-steady state solution.

3. General trends

Figs 1 and 2 show a range of normalized radius–time curves for the diffusion controlled dissolution of spheres obtained by these finite difference methods; the corresponding times needed for dissolution are given in Table I. A typical radius–time curve first shows a decrease in rate of change of size but an increase in the latter stages; the inflexion occurs quite early for small values of the effective solubility F_d but is found in only the last stages for large values of F_a. Comparison of the results given in Table I with those given by Cable and Evans [9] shows that the computing methods used in that work were insufficiently refined even for low solubilities because a very accurate estimate of concentration gradient at the interface is required.

Fig. 1 shows results for $\varepsilon = 1$, that is, no change in the volume of the solution, and is thus typical of gas bubbles. Fig. 2 shows results for $\varepsilon = 0$ which corresponds to the volume of the whole system remaining

TABLE I Dimensionless times (z_d) for complete dissolution of a sphere

F_a	ε		
	0	0.5	1
0.001	486.6	486.5	486.4
0.01	46.48	46.40	46.25
0.1	4.214	4.106	3.994
0.2	2.057	1.953	1.846
0.05	0.834	0.742	0.644
1	0.451	0.3707	0.2828
2	0.2670	0.1987	0.1214
5	0.1536	0.1003	0.03861
10	0.1111	0.0669	0.01599
20	0.0855	0.0483	0.00656
50	0.0651	0.03473	0.002006
100	0.0546	0.02835	0.000814

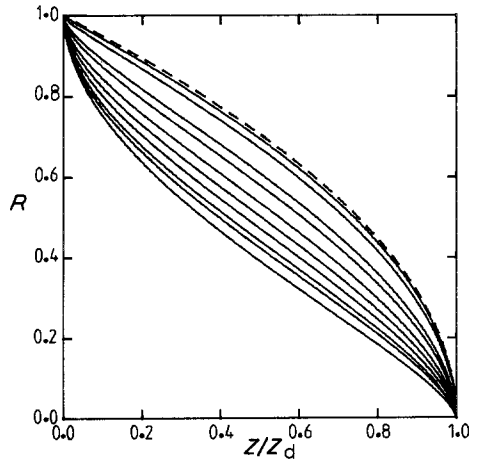

Figure 2 Normalized radius–time curves for $\varepsilon = 0$ and $F_a = 0.001$, 0.01, 0.1, 0.2, 0.5, 1, 2, 5, 10 and 100, the dashed line shows the quasi-steady state solution.

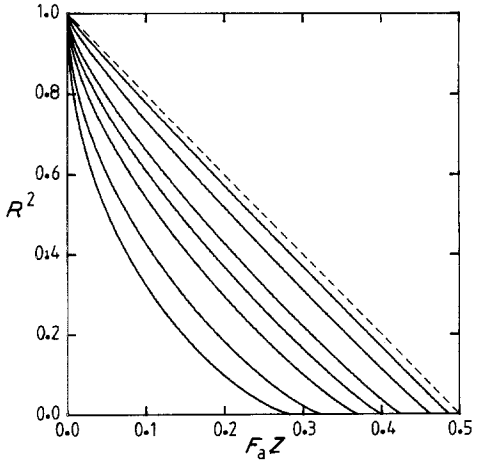

Figure 3 The steadily increasing deviation from the quasi-steady state approximation (dashed line) as solubility increases. $\varepsilon = 1$, $F_a = 0.0001$, 0.01, 0.05, 0.1, 0.2, 0.5 and 1 (reading from top to bottom).

constant and may be considered a reasonable approximation for the dissolution of many solids. Table I shows that the value of ε has little effect on the time for complete dissolution when solubility is small ($F_a < 0.01$) but has a growing influence as F_a increases above 0.1, the effect becoming very large at high values.

The normalized curves shown in Figs 1 and 2 suggest that the solutions tend to a unique regime for very small solubility (F_a); this is discussed in the next section. Fig. 1 does not suggest any approach to a typical regime for large F_a except to indicate that the initial stage becomes increasingly faster than the last stages. Understanding of these trends must take into account the spherical symmetry of the system and the role of radial convection which competes with diffusion in determining the evolution of the concentration profiles for moderate and high solubilities. Enhancement of rate of dissolution during the final stage, which occurs in all cases, is not expected of solutions based on the behaviour of spheres of constant size or results for growing spheres when the possible influence of surface tension is neglected.

4. Limiting solutions

The limiting quasi-steady state solution for very small F_a is readily obtained by neglecting convection and accumulation close to the interface. As either dR/dz or $\partial F/\partial e$ becomes very small the convective term in Equation 3, $\varepsilon(R/e)^2(dR/dz)\partial F/\partial e$, also becomes very small and may be neglected. Thus Equation 3 becomes

$$\frac{1}{e^2}\frac{\partial}{\partial e}\left[e^2\frac{\partial F}{\partial e}\right] = 0 \qquad (5)$$

and on integrating from $e = R$, $F = F_a$,

$$\left(\frac{\partial F}{\partial e}\right)_R = \frac{-F_a}{R}, \qquad (6)$$

$$F = F_a(R/e); \quad e \geqslant R. \qquad (7)$$

Combining Equations 4 and 6 thus leads to

$$R^2 = 1 - 2F_a z \qquad (8)$$

and some of the results already given are replotted in this form in Fig. 3; it is seen that Equation 8 is good only for $F_a < 0.001$.

Duda and Vrentas [10] used a quasi-steady state approximation which includes the effect of convection; their solution reduces to

$$R^2 = 1 - 2\left[\frac{\ln(1 + (1 - \varepsilon))}{1 - \varepsilon}\right]F_a z \qquad (9)$$

However, the quasi-steady state approximation applies only to quite low solubilities ($F_a < 0.01$), for which Equations 8 and 9 are almost the same and convection unimportant. This is also shown by Table I where it is seen that times to dissolve are almost independent of ε for $F_a < 0.01$.

With $F_a > 0.1$ the deviations from the quasi-steady state solution become distinctly dependent on the value of F_a, indicating the possibility of estimating both solubility and diffusivity from sufficiently accurate experimental data, as suggested by Brown and Doremus [13]. This is not possible for small values of F_a because the shape of the normalized radius–time curve is insensitive to F_a.

Intuition may suggest that the behaviour for sufficiently large F_a should approach that of a flat slab because the concentration profile will occupy a distance much smaller than R. According to Crank [12]. this is

$$R = 1 - 2F_a\sqrt{z/\pi} \qquad (10)$$

Computed results for moderate and large values of F_a and $\varepsilon = 1$ are plotted in this form in Fig. 4; it is seen that the flat slab approximation is reasonable for $1 > R > 0.8$ in all cases and this represents dissolution for nearly half the total mass. However, this approximation neglects the increase in the volume of solution with increasing radius and thus predicts slower dissolution than the proper solution for low and moderate solubilities because of the effect on the concentration profile. On the other hand, the flat slab model predicts excessively fast dissolution for large F_a because it ignores the accumulation of solute near the interface imposed by the rapidly decreasing size of the sphere and the consequent inevitable increase in boundary layer thickness. During the early stage diffusion occurs in only a thin boundary layer, which accounts

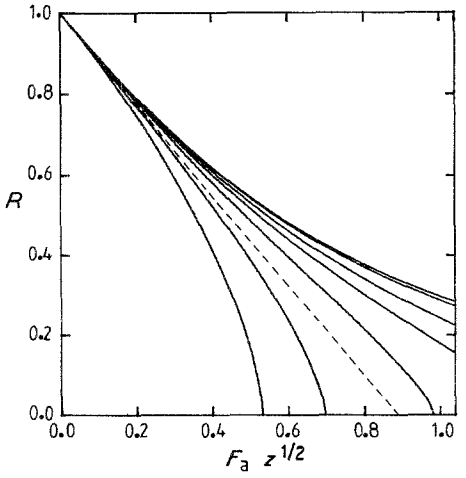

Figure 4 Deviations from the flat slab approximation (dashed line) for $\varepsilon = 1$ and $F_a = 1000, 100, 20, 10, 5, 2$ and 1 (reading from top to bottom).

for the agreement with the flat slab model, and this happens because the velocity in the boundary layer

$$u(r) = \varepsilon(a/r)^2 \mathrm{d}a/\mathrm{d}t, \qquad (11)$$

depends only on time provided that $(r - a) \ll a$.

If $\varepsilon \neq 1$ the volume of the solution changes with time and there is a discontinuity in velocity at the interface, that is $u(a) \neq \mathrm{d}a/\mathrm{d}t$. The flat slab approximation thus becomes increasingly poor as ε departs from unity.

Fig. 4 also shows that for very high solubility ($F_a > 100$) the normalized radius curves tend to converge to a common form when plotted against $F_a z^{1/2}$, at least for $R > 0.4$, but this does not correspond to any obvious approximation.

The quasi-stationary approximation is based on the concentration distribution developed around a sphere of constant radius [5], which makes the concentration gradient at the surface of the sphere a function of both time and sphere radius. When combined with Equation 4 this gives

$$\mathrm{d}R/\mathrm{d}z = -F_a\left(\frac{1}{R} + \frac{1}{\sqrt{\pi z}}\right) \qquad (12)$$

For sufficiently short times and small values of boundary layer thickness (large F_a) this becomes identical with the flat slab model (Equation 10): for very small solubility, hence very long times, Equation 8 results. Fig. 5 shows how the times for complete dissolution given by the flat slab, quasi-steady state and quasi-stationary approximations compare with those given by the full numerical solutions for $\varepsilon = 1$. It is clear that none of these approximations is very useful over the range of solubilities often of interest, ($F_a > 0.01$) but both the steady state and stationary models are acceptable for very small solubilities. The fact that two of the results converge for $F_a > 50$ does not show them to be correct in that range.

5. Concentration distributions

Analysis of concentration profiles helps to understand the development of boundary layers and the factors likely to influence their evolution. Fig. 6 shows concentration distributions typical of very low F_a; the dashed lines show the quasi-steady state predictions and the full lines the computed numerical results. The two sets of curves always agree well close to the interface although some differences are usually seen in the tails. However, the two curves are almost identical for $R = 0.5$. This approximation thus gives reliable predictions of $R(z)$ for very low solubility, the concentration gradient at the interface increasing steadily as size decreases according to Equation 6.

With large values of solubility (F_a), solute accumulates close to the interface and the radial convection produces some features not expected in Fickian diffusion. Fig. 7 shows computed concentration profiles for a dissolving sphere with $F_a = 10, \varepsilon = 1$. When the sphere has become quite small, $R \leqslant 0.25$, the profiles show inflexions (the second derivative of concentration becomes negative) near the interface. This results from the forced contraction of the volume of the reservoir available to contain the solute already transferred to the solution as the sphere shrinks. This effect has not been seen with other geometries or spheres of either constant or increasing size. The way in which space and time mesh sizes are automatically adjusted periodically guarantees that these unexpected

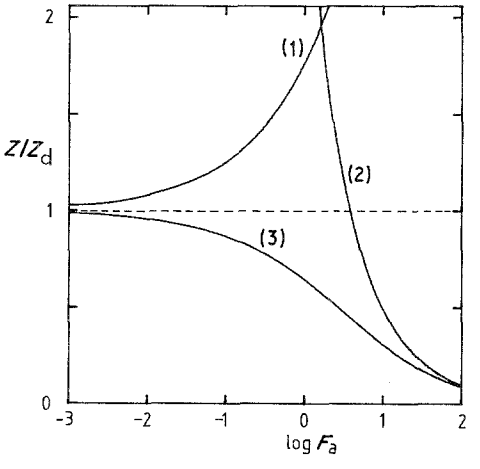

Figure 5 Comparison of computed times to dissolve (z_d) with the predictions (z') given by (1) quasi-steady state, (2) flat slab and (3) quasi-stationary approximations for $\varepsilon = 1$.

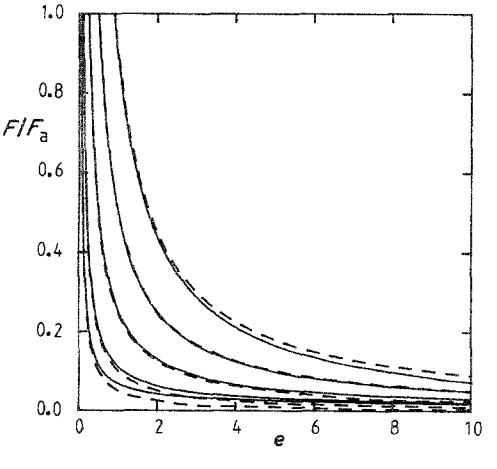

Figure 6 Comparison of concentration profiles at various stages of dissolution, from right to left $R = 0.9, 0.5, 0.25, 0.1$, and 0.05, for $\varepsilon = 1$, $F_a = 0.0001$. —— Computed results, – – – quasi-steady state.

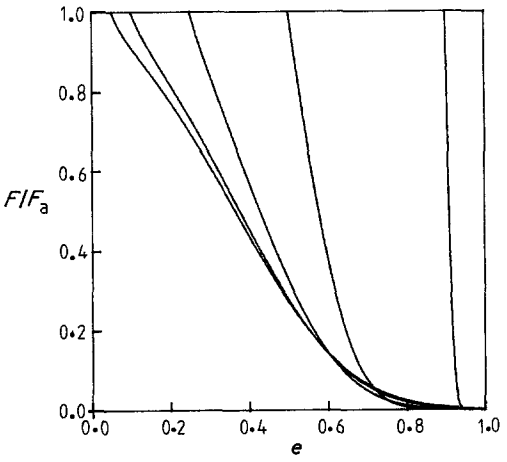

Figure 7 Computed concentration profiles at various stages of dissolution, from right to left R = 0.9, 0.5, 0.25, 0.1 and 0.05, for $\varepsilon = 1$, $F_a = 10$.

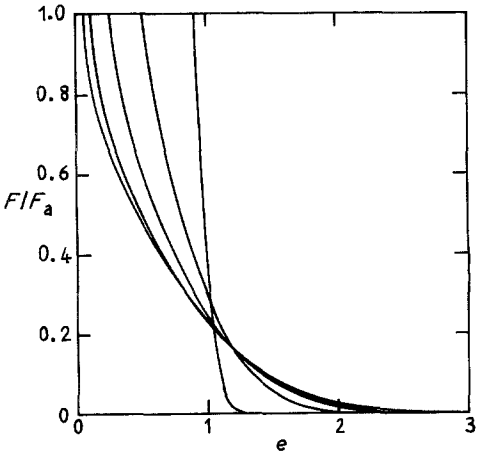

Figure 9 Computed concentration profiles for $\varepsilon = 1$, $F_a = 1$ at radii (from right to left) R = 0.9, 0.5, 0.25, 0.1 and 0.05.

features of the concentration profiles are not due to errors in the finite difference procedures used here.

Confirmation that radial convection can be responsible for inflexions in concentration profiles is shown in Fig. 8 for $F_a = 100$. If transport of solute were exclusively due to convection a point at which concentration $F_1 = F(e_1, R_1)$ was originally at e_1 would move to e_2 when radius of the sphere decreased from R_1 to R_2 according to the relation

$$e_1^3 - R_1^3 = e_2^3 = R_2^3, \tag{13}$$

so that

$$e(F_1) = [e_1^3 - R_1^3 + R^3]^{1/3} \tag{14}$$

The dashed curves in the Fig. 8 show the effect of radial convection alone, calculated using this relation, on the concentration profile for $R = 0.25$ when the radius has further decreased to $R = 0.1$ and 0.05. These curves show an inflexion and differ only a little from the profiles computed for these radii by the full numerical solution, including diffusion, which are shown by full lines. This extreme case clearly demonstrates that the accumulation of solute near the interface imposed by radial convection is largely responsible for the increasingly slower later stage seen in Fig. 2 when solubility becomes very large ($F_a > 10$). For $F_a = 1000$ and $\varepsilon = 1$ the sphere shrinks to $R = 0.1$ in only about 11% of the time needed for complete dissolution.

The quasi-steady state solution (Equation 7) illustrates the role of spherical geometry for very low solubility for which it makes the concentration gradient at the interface nearly proportional to $1/R^2$ so that the rate of dissolution keeps increasing as the sphere shrinks.

For intermediate values of solubility, especially $0.1 < F_a < 10$, the concentration profiles show a progressive transition. At first behaviour is similar to a flat slab but later becomes increasingly affected by radial convection. A typical case is shown in Fig. 9 and no qualitatively unexpected features are seen.

For $\varepsilon < 1$ the volume of the solution increases as dissolution proceeds and this extra factor contributes to expansion of the boundary layer. When $\varepsilon = 0$ the liquid remains motionless but the movement of the boundary distorts the concentration profiles that diffusion alone might be expected to produce. Fig. 10 shows that this is sufficient to cause inflexions in the concentration profiles for large F_a. Note that an inflexion already exists for $R = 0.9$. The evolution of concentration profiles lies between the extremes already discussed for $0 < \varepsilon < 1$. If ε should be negative radial convection would play an even greater part

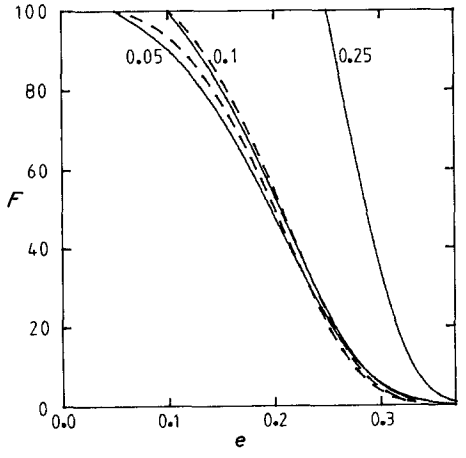

Figure 8 Computed concentration profiles at R = 0.25, 0.1 and 0.05 for $\varepsilon = 1$, $F_a = 100$. The dashed lines show the effect of radial convection alone on the profile for $R = 0.25$.

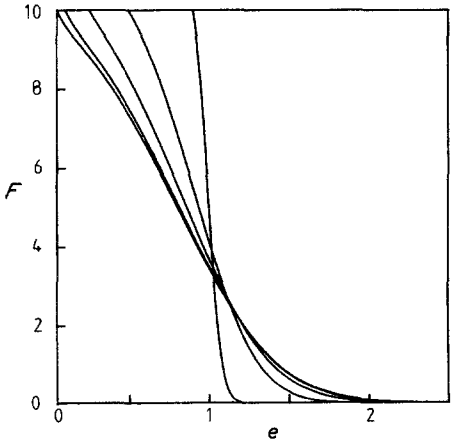

Figure 10 Computed concentration profiles for $\varepsilon = 0$, $F_a = 10$ at radii (from right to left) R = 0.9, 0.5, 0.25, 0.1 and 0.01.

because the liquid would then flow in the opposite direction to the movement of the interface.

The examples given in Figs 7, 8 and 10 show that concentration profiles of sigmoidal shape do not necessarily imply that a process is controlled by non-Fickian diffusion [14] or that diffusivity is strongly concentration dependent.

6. The design of experiments

The medium surrounding the sphere has been assumed infinite: this is experimentally both unattainable and undesirable. It is usual to make experimental systems as small as possible to minimize the development of accidental bulk convection as well as to aid manipulation and observation. It is therefore desirable to establish criteria for selecting the minimum size of the whole system relative to the initial size of the sphere. The criterion chosen was the radius at which the dimensionless concentration had increased by 1% when the sphere had shrunk to $R = 0.05$; these results are shown in Table II. The size of the spherical shell (r^*/a_0) needed to accommodate the diffusion field increases as solubility decreases and, for high solubility, as ε decreases. These results do not impose serious problems in the design of experiments except for $F_a < 0.1$. This criterion does not consider the development of the spherically symmetrical velocity field which would require a larger volume. For example, dissolution of a gas bubble, $\varepsilon = 1$, would cause a 12.5% change in the volume of the whole system if its initial size were only twice as big as the initial bubble and using a cylinder with $r^*/a_0 = 2$ might not be satisfactory even for $F_a = 2$.

7. Conclusion

Although analytical solutions are possible for growth of spheres from zero initial size, no such solutions are possible for growth or dissolution from finite initial size. Accurate and versatile numerical methods have therefore been developed to solve the differential equations describing these cases. The techniques used were designed to function efficiently for either growth or dissolution and for very wide ranges of the relevant parameters. Extensive tests of computed results for growing spheres against the analytical results for size as a function of time and also the concentration distributions have already been reported. The excellent agreement found is considered sufficient evidence that the numerical procedures developed are accurate for dissolution as well as growth. The main features of the numerical solutions for the diffusion controlled dissolution of isolated spheres are therefore reported here. Time transient effects generally persist throughout the whole course of dissolution and, as a result, there are no generally valid approximations for radius–time curves, times to dissolve completely, or concentration distributions: this is a marked contrast to the behaviour of growing spheres. Figs 1 and 2 together with Table I allow the predicted behaviour of a wide range of important cases to be deduced.

TABLE II Estimated size (r^*/a_0) of the shell needed to accommodate the diffusion field of a dissolving sphere

F_a	ε	
	0	1
0.01	13.7	13.7
0.02	11.1	10.9
0.05	7.81	7.77
0.1	6.03	5.93
0.2	4.70	4.48
0.5	3.47	3.06
1	2.86	2.28
2	2.45	1.69
5	2.11	1.14
10	1.95	< 1

For sufficiently low solubilities, $F_a = 0.001$, a quasi-steady state solution is valid but no simple approximation is very useful for higher solubilities. A flat slab model fails for high solubilities except during a relatively short initial stage, $1 > R > 0.8$. The frequently used analogy between heat conduction [15] and mass transfer is not generally applicable to dissolution because it entirely neglects the important effects of radial convection and motion of the boundary. Examination of concentration profiles developed during dissolution has shown that inflexions can be produced by the radial convection and motion of the boundary accompanying dissolution, although no such inflexions occur for spheres of constant or increasing size with equivalent parameters. The development of sigmoidal concentration distributions around dissolving spheres thus does not demonstrate that diffusion is non-Fickian or that diffusivity is strongly concentration dependent but is due to the influence of spherical geometry. The effects of concentration-dependent diffusivity will be reported elsewhere [3].

The partial molar volume of the solute in the solution has trivial effects for very small solubilities but becomes increasingly important as solubility increases and must be taken into account for moderate and high solubilities ($F_a > 0.1$) if accurate results are required.

Acknowledgements

The University of Aveiro, Portugal, (Department of Ceramic Engineering and Glasses) is warmly thanked for giving J. R. Frade leave of absence to undertake this work. The Calouste Gulbenkian Foundation generously provided additional financial assistance.

References

1. L. E. SCRIVEN, *Chem. Eng. Sci* **10** (1959) 1.
2. M. CABLE and J. R. FRADE, *J. Mater. Sci.* **22** (1987) 919.
3. *Idem, Chem. Engng Sci.* submitted.
4. *Idem, J. Mater. Sci.* **22** (1987) 149.
5. P. S. EPSTEIN and M. S. PLESSET, *J. Chem. Phys.* **18** (1950) 1505.
6. I. M. KRIEGER, G. W. MULHOLLAND and C. S. DICKEY, *J. Phys. Chem.* **71** (1967) 1123.
7. J. L. DUDA and J. S. VRENTAS, *Amer. Inst. Chem. Eng. J.* **15** (1969) 351.
8. D. W. READEY and A. R. COOPER, *Chem. Eng. Sci.* **21** (1966) 917.
9. M. CABLE and D. J. EVANS, *J. Appl. Phys.* **38** (1967) 2899.
10. J. L. DUDA and J. S. VRENTAS, *Int. J. Heat Mass Transfer* **14** (1971) 395.
11. J. R. FRADE, PhD thesis, Sheffield University, 1983.

12. J. CRANK, "The mathematics of diffusion" 2nd edn (Clarendon, Oxford, 1975) Ch. 3.
13. R. B. BROWN and R. H. DOREMUS, *J. Amer. Ceram. Soc.* **59** (1976) 510.
14. J. CRANK, "The mathematics of diffusion", 2nd edn (Clarendon, Oxford, 1975) Ch. 11.
15. H. S. CARSLAW and J. C. JAEGER, "The conduction of heat in solids", 2nd edn (Clarendon, Oxford, 1959) Ch. 9.

Received 11 September
and accepted 8 December 1986